

## Strongly Enhanced Backward Emission of Electrons in Transfer and Ionization

M. Schulz,<sup>1,2</sup> X. Wang,<sup>3,4</sup> M. Gundmundsson,<sup>5</sup> K. Schneider,<sup>3,6</sup> A. Kelkar,<sup>3,6</sup> A. B. Voitkiv,<sup>3</sup> B. Najjari,<sup>3</sup> M. Schöffler,<sup>2</sup>  
L. Ph. H. Schmidt,<sup>2</sup> R. Dörner,<sup>2</sup> J. Ullrich,<sup>3</sup> R. Moshhammer,<sup>3</sup> and D. Fischer<sup>3</sup>

<sup>1</sup>*Physics Department and LAMOR, Missouri University of Science & Technology, Rolla, Missouri 65409, USA*

<sup>2</sup>*Institut für Kernphysik, Universität Frankfurt, Max-von-Laue Strasse 1, D-60438 Frankfurt, Germany*

<sup>3</sup>*Max-Planck-Institut für Kernphysik, Saupfercheckweg 1, D-69117 Heidelberg, Germany*

<sup>4</sup>*Shanghai EBIT Laboratory, Institute of Modern Physics, Fudan University, Shanghai 200433, China*

<sup>5</sup>*Stockholm University, Atomic Physics, Alba Nova, S-106 91 Stockholm, Sweden*

<sup>6</sup>*Extreme Matter Institute EMMI, GSI Helmholtzzentrum für Schwerionenforschung GmbH,  
Planckstraße 1, D-64291 Darmstadt, Germany*

(Received 20 October 2011; published 26 January 2012)

We studied three-dimensional angular distributions and longitudinal momentum spectra of electrons ejected in transfer plus ionization (TI), i.e., the ejection of one and the capture of a second target electron, for ion-helium collisions. We observe a pronounced structure strongly focused opposite to the projectile beam direction, which we associate with a new correlated TI mechanism proposed recently. This process contributes significantly to the total cross sections over a broad range of perturbations  $\eta$ , even at  $\eta$  as large as 0.5, where uncorrelated TI mechanisms were thought to be dominant.

DOI: [10.1103/PhysRevLett.108.043202](https://doi.org/10.1103/PhysRevLett.108.043202)

PACS numbers: 34.70.+e, 34.50.Fa

One of the most pressing goals of research in atomic collisions is to advance our understanding of the few-body problem (FBP) (e.g. [1,2]). The essence of the FBP is that the equations of motion are not analytically solvable for more than two interacting particles even when the underlying forces are precisely known. In this context, single ionization (SI) of atoms by charged-particle impact, representing one basic manifestation of the FBP, has been studied extensively (for reviews see, e.g., [3,4]). In particular, fully differential measurements have advanced our understanding of the underlying collision dynamics [1,4]. Here, three-dimensional angular distributions of the ejected electrons for fixed momentum transfer  $q$  (difference between the initial and final projectile momentum) and electron energy are obtained. While for slow collisions the spectra are quite rich in structure [5,6], the main features for fast collisions are relatively simple consisting of a double lobe structure: A large peak, the binary peak, is usually observed approximately in the direction of  $q$  and a smaller peak, the recoil peak, in the direction of  $-q$ . Such fully differential data are at least qualitatively well reproduced by theory, although for specific kinematic regimes puzzling discrepancies continue to persist (e.g., [1,7]).

More recently the focus in tackling the FBP has shifted towards two-electron transitions like, e.g., double ionization (DI) (e.g., [8–12]), double excitation (e.g., [13]), double capture (e.g., [14,15]), or transfer plus ionization (TI) (e.g., [16–20]). One might expect that the dynamics of these reactions differs significantly from one-electron transitions, such as SI, because of the increased importance of electron-electron correlations [21] and because a larger final-state phase space is available for two active electrons. Nevertheless, amazing similarities between DI and SI

were obtained in so far as the characteristic binary-recoil double lobe structure, well-known from SI studies, was observed in the three-dimensional angular distribution of the sum momentum of both electrons ejected in double ionization [22].

TI, i.e., ionization accompanied by the capture of a second target electron by the projectile, is particularly suitable to compare the collision dynamics between two- and one-electron transitions. This process bears more resemblance to SI than DI in so far as the final-state involves only one-electron in the continuum. Thus, one can directly compare the final continuum state of the ejected electron with and without the condition that a second electron is captured by the projectile. If the capture of the second electron is assumed to be largely independent of the ejection of the first electron (independent TI) one would expect that the three-dimensional angular distribution of the ejected electron is even more similar to SI than the one of the sum momentum of both electrons ejected in DI. On the other hand, at large projectile energies correlation between the captured and the ejected electron is believed to be quite important. The nature of this correlation has been the subject of vivid discussions (e.g., [16–20,23]). One assertion that has caught particular interest is that experimental data on TI could reveal the small non- $s^2$  contribution in the correlated ground-state wave function of helium [23]. However, recently a new correlated TI process has been proposed [24] and in this mechanism these contributions are not very important.

In this Letter we report measured three-dimensional angular distributions of electrons ejected in TI. Major qualitative differences to SI are observed, which cannot be explained in terms of an independent TI mechanism.

Instead, the data are qualitatively reproduced by calculations which are based on the new correlated TI mechanism [24] mentioned above. Considering the relatively large perturbation parameters  $\eta$  of up to 0.5 (projectile charge to speed ratio) of the investigated collision systems, the contributions from this correlated process, which was completely overlooked in decades of research on TI, are surprisingly large.  $\eta$  represents a crude criterion whether the interaction potential can be viewed as a small perturbation relative to the unperturbed potential. As a rule of thumb this is not the case, and higher-order contributions become important, if  $\eta$  is not small compared to unity.

The experiments were performed at the ion storage ring of the Max-Planck-Institut für Kernphysik in Heidelberg [25] with 1 MeV/amu  $\text{Li}^{3+}$  projectiles, and at the Institut für Kernphysik of the University of Frankfurt with 630 keV/amu  $p$ ,  $\text{He}^+$ , and  $\text{He}^{2+}$  projectiles. In all cases, the width of the beams was less than 1 mm. The projectile beam was crossed with a cold ( $T \lesssim 2$  K) neutral helium beam from a supersonic jet. The charge-exchanged projectiles were selected by a dipole magnet (electrostatically in the Frankfurt experiments) and detected by a scintillation detector or a position-sensitive micro-channel plate detector. Electrons and recoil ions produced in the collision were extracted by an electric field of about 18(4.8) V/cm for the  $\text{Li}^{3+}$  ( $p$ ,  $\text{He}^{+,2+}$ ) projectiles and detected by two-dimensional position-sensitive micro-channel plate detectors. Both spectrometers are very similar and described in detail elsewhere [26,27]. They differ, however, in the extraction direction, which is perpendicular to the projectile beam in the Frankfurt experiment and longitudinal, i.e., parallel to the projectile beam, in the Heidelberg experiment. Electrons with momentum components in the plane perpendicular to the extraction field of less than 2 (5) atomic units (a.u.) were guided onto the detector by a uniform magnetic field of 12 (21) G.

The detectors for all three collision fragments were operated in coincidence. TI events are unambiguously identified by true triple coincidences between a charge-exchanged projectile, a  $\text{He}^{2+}$  recoil-ion, and an ejected electron. Using the two-dimensional position and coincidence time information the electrons and the recoil ions were fully momentum-analyzed. The momentum transfer  $q$  from the projectile to the target fragments is then already determined from momentum conservation by  $q = \mathbf{p}_{\text{el}} + \mathbf{p}_{\text{rec}} + v_0$  (where  $v_0$  is due to the momentum of the captured electron). The momentum resolution for the recoil ions was 0.5–0.7 a.u. in the case of the  $\text{Li}^{3+}$  projectiles and 0.15 a.u. for the other projectiles. The somewhat restricted resolution for the  $\text{Li}^{3+}$  data (due to the relatively large extraction field) does not represent a significant limitation on the experiment because TI leads to much larger recoil-ion momenta than, e.g., SI or even DI. The electron resolution was better than 0.1 a.u. FWHM for all components and for all projectiles.

Before presenting the measured three-dimensional angular distributions of electrons ejected in TI (in the following simply called 3D plots), we first compare in Fig. 1 theoretical 3D plots for electrons ejected in SI [1(a)] and in independent TI [1(b)] in 1 MeV/amu  $\text{Li}^{3+} + \text{He}$  collisions. The arrow labeled  $\mathbf{p}_0$  indicates the initial projectile beam direction and the plane of the paper coincides with the scattering plane defined by  $\mathbf{p}_0$  and  $q$  (which for SI is given by  $q = \mathbf{p}_{\text{el}} + \mathbf{p}_{\text{rec}}$ ), where  $q$  always lies in the right half of the scattering plane (Although the data of Fig. 1 are integrated over all magnitudes of  $q$  its azimuthal angle, i.e., the direction of its transverse component  $q_r$ , was determined in the data analysis for each event. The azimuthal angle of the ejected electron was measured with respect to  $q_r$ . Figure 1 contains the data for all directions of  $q$ . The arrow labeled  $q$  in Fig. 1 schematically indicates the average direction of  $q$ ). The SI cross sections were calculated within the continuum distorted wave—eikonal initial state approach [28] and the TI cross sections were obtained by convoluting SI and electron capture amplitudes, where the latter was calculated within the continuum distorted wave [29]. The interaction between the nuclei of both collision

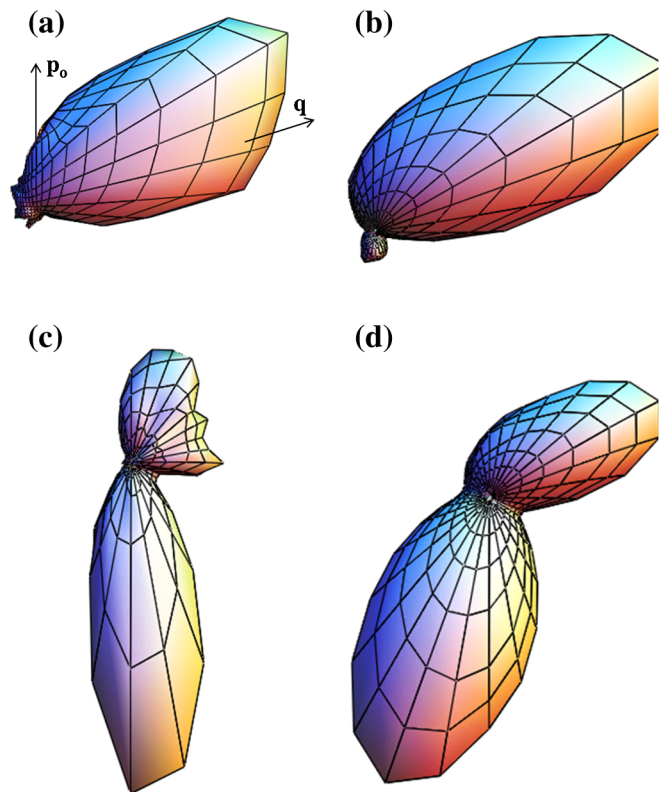


FIG. 1 (color online). Three-dimensional angular distribution of electrons ejected in 1 MeV/amu  $\text{Li}^{3+} + \text{He}$  collisions. (a) Calculation for electrons ejected in single ionization; (b) calculation for electrons ejected in independent transfer ionization; (c) experimental data for electrons ejected in transfer-ionization; (d) calculation for electrons ejected in the independent and  $ee$  transfer-ionization processes.

partners (nn interaction) was incorporated by means of the eikonal approximation [30]. The spectra for SI and independent TI are qualitatively quite similar. For SI the well-known binary-recoil double lobe structure (although the recoil peak is very weak), which has also been observed in experimental data for similar collision systems [4], is visible. For independent TI a pronounced binary peak, very similar to the one observed in SI, is present as well. The only significant difference is that instead of the recoil peak a very small structure in the direction of  $-\mathbf{p}_0$  is seen.

In Fig. 1(c) we show an experimental 3D plot for electrons ejected in TI in 1 MeV/amu  $\text{Li}^{3+}$  collisions. Significant and qualitative differences to the theoretical results for independent TI are quite obvious. Although a small binary peak is present, the most prominent feature in the measured data is now a large and narrow peak in the direction of  $-\mathbf{p}_0$ . Thus, the comparison to theory strongly suggests that the dynamics of TI is very different from the one for SI and that some mechanism other than independent TI must be important.

Processes in which the ionization and capture steps are correlated with each other, such as the shake process [31] or the Thomas mechanism of the second kind [16,18,32,33], were thought to contribute only a small fraction to the total TI cross sections at  $\eta$  as large as studied here. In both processes, the transition of only one electron is caused by a direct interaction with the projectile. In the shake process, the transition of the second electron is caused by a change of the eigenstates of the target Hamiltonian triggered by the transition of the first electron, which can be regarded as an initial-state correlation effect. In the Thomas mechanism of the second kind, a direct collision between both electrons (after the interaction of the projectile with the first electron) leads to the transition of the second electron.

Very recently, a new correlated TI mechanism, dubbed the  $ee$  process, has been suggested [24,29], for which the  $\eta$  dependence has not been systematically studied yet. The  $ee$  TI process is perhaps best described in the rest frame of the projectile, where it can be viewed in analogy to radiative capture. Here, the target electron undergoes a transition from a quasicontinuum state, highly excited due to the relative motion between the projectile and the electron, to a projectile bound state. In the  $ee$  process the excess energy is not transferred to a photon, but instead mainly to a second target electron, which thereby gets ejected in the backward direction (in the target rest frame), thus, completing the TI process. In this description, the  $ee$  mechanism can be regarded as an Auger decay of a two-electron quasicontinuum state.

In Fig. 1(d), we show a calculated 3D plot of electrons ejected in TI in 1 MeV/amu  $\text{Li}^{3+}$  collisions, where the contributions from the independent and the  $ee$  processes were added incoherently. The theoretical method to calculate the cross sections for the  $ee$  process has been described

earlier [29]. Large differences to the theoretical plot for the independent process alone are quite obvious. In addition to the binary peak a pronounced structure in the backward direction emerges and is now the most prominent feature in the 3D plot. Including the  $ee$  process in the calculation drastically improves the agreement with the experimental data; most notably the backward peak is qualitatively reproduced. Nevertheless, some quantitative discrepancies remain. The binary peak is overestimated by theory and the location of the backward peak in the polar angle  $\theta_e$  (measured relative to  $\mathbf{p}_0$ ) differs by about  $25^\circ$  from the experimental data. However, in spite of these shortcomings, which might be due to the incoherent summation of amplitudes, we conclude that the narrow backward peak is a clear signature of the  $ee$  process.

A large flux of electrons with negative longitudinal momentum components has been observed for TI in  $p + \text{He}$  collisions earlier [19], but there the electrons had at the same time a relatively large transverse momentum. Therefore, the data did not exhibit a structure as strongly focused in the direction of  $-\mathbf{p}_0$  as we observe here. However, it should be noted that in that experiment the electrons were not detected. Instead, the momenta of the recoil ions and charge-exchanged projectiles were measured and the electron momentum was deduced from momentum conservation. The relatively poor resolution in the projectiles was reflected in the electron resolution as well and resulted in electron momenta which were too large both in the longitudinal and transverse directions. This, in turn, led to a significant artificial shift of the electron distribution away from the  $-\mathbf{p}_0$  direction. In the present experiment, the electron momentum was measured directly resulting in a much better resolution. With this improved resolution, we now observe for the  $p$  and  $\text{He}^{+,2+}$  projectiles electron emission as strongly focused in the  $-\mathbf{p}_0$  direction as for the  $\text{Li}^{3+}$  projectiles.

The 3D plots already qualitatively show that the  $ee$  process is a strong contributor to TI even at this relatively large  $\eta$ . In order to study the relative importance of the independent and  $ee$  contributions quantitatively as a function of the projectile charge  $Q$  and speed  $v_0$ , we present longitudinal momentum spectra of the ejected electrons for  $p$ ,  $\text{He}^+$ ,  $\text{He}^{2+}$ , and  $\text{Li}^{3+}$  projectiles in Fig. 2(a)–2(d). The data were not absolutely normalized, and for each collision system we adjusted the magnitude to give the best overall fit with theory. Two components, although not fully resolved, can be identified in these plots, one occurring at negative and one at positive longitudinal momenta. Based on the discussion of the 3D plots it is clear that the former can be associated mostly with the  $ee$  process and the latter with the independent process. Comparing the data for  $p$  and  $\text{He}^+$  impact shows that the intensity ratio for both contributions does not follow a simple scaling with  $\eta$ . Although  $\eta$  has the same value for both projectiles the spectra are very different, where for  $p$  impact the

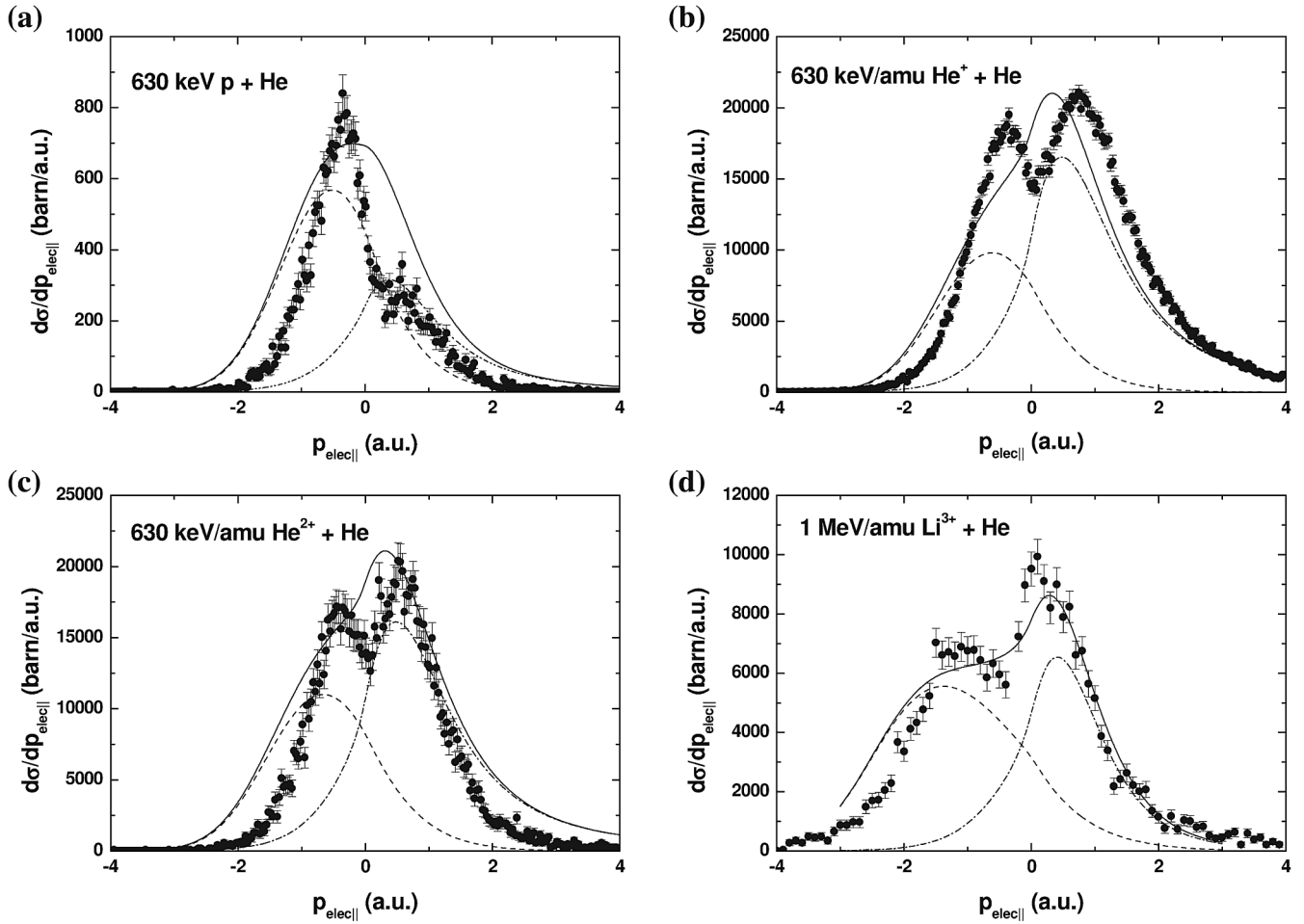


FIG. 2. Longitudinal momentum spectra of electrons ejected in transfer ionization in (a) 630 keV  $p + \text{He}$ ; (b) 630 keV/amu  $\text{He}^+ + \text{He}$ ; (c) 630 keV/amu  $\text{He}^{2+} + \text{He}$ ; (d) 1 MeV/amu  $\text{Li}^{3+} + \text{He}$ . The dashed and dash-dotted curves are calculations for the  $ee$  and independent transfer-ionization processes, respectively, and the solid curve is the incoherent sum of both contributions.

contributions from the independent process are rather small while for  $\text{He}^+$  impact they are of similar magnitude. This illustrates that the binding energy of the captured electron in the projectile or the screening of the nuclear charge in  $\text{He}^+$ , which are the only significant differences between both collision systems, plays a crucial role in the relative importance between the independent and the  $ee$  processes. For all projectiles the contributions from the  $ee$  mechanism are similar to those from the independent process or even larger. This may seem surprising since, in general, correlated two-electron processes tend to become weaker relative to independent mechanisms with increasing  $\eta$  and are usually insignificant at values as large as 0.5. In contrast, the  $ee$  process remains important even for the  $\text{He}^{2+}$  and  $\text{Li}^{3+}$  projectiles, for which  $\eta = 0.4$  and 0.5, respectively. However, viewing  $ee$  TI as an Auger decay of a two-electron quasicontinuum state, as described above, makes these relatively large contributions understandable: the corresponding Auger transition matrix element is a first-order amplitude involving a large spatial

overlap of the electrons in the initial correlated ground state of helium.

The dashed and dash-dotted curves in Fig. 2 are our calculations of the contributions from the  $ee$ —and independent processes to the longitudinal electron momentum spectra—and the solid curves represent the incoherent sum of both. Qualitatively, the experimental spectra are well reproduced by the calculations. In particular, with the exception of the  $\text{He}^+$  case, the calculated peak position for each process and their relative magnitudes are consistent with the measured data. On the other hand, especially the peak structure for  $ee$  TI is significantly broader than in the experiment. Furthermore, in the experimental data (except for the proton projectiles) the  $ee$  and independent contributions are separated by a minimum, which is not seen in the calculations. This could be due to destructive interference between both contributions, which is not accounted for by theory because it treats them incoherently. Since the amplitudes for both processes are calculated in two independent codes it is currently not feasible to

compute the relative phase factor which is needed for a coherent treatment.

In summary, we have presented longitudinal momentum spectra and, for the first time, three-dimensional angular distributions of electrons ejected in TI. We observe a surprisingly intense and strongly focused emission in the backward direction. Furthermore, a weaker binary peak, similar to what is routinely observed for SI, is found. The backward peak is a characteristic signature of a recently proposed correlated TI mechanism ( $ee$  process), in which non- $s^2$  contributions in the correlated initial target-state are not needed. The binary peak is due to ionization accompanied by uncorrelated capture. Our data not only provide experimental evidence for the  $ee$  process, but moreover they demonstrate that it contributes a significant fraction of TI cross sections over a broad range of different collision systems. In this context, it is remarkable that it has been overlooked in decades of research on TI. However, we expect that the  $ee$  process will be small compared to the independent process for slow collisions [5] and for highly charged ions at relatively small velocities, where the single capture cross sections are very large. Furthermore, the relative importance of this mechanism for more complex targets is not clear. Depending on the state from which the electrons are removed from the target, initial-state correlation could be weaker or stronger than in helium, which could have a significant effect on the ratio between correlated and uncorrelated TI mechanisms. Experiments studying TI for a lithium target are currently in preparation. As for a theoretical outlook, a new code which computes the amplitudes for the  $ee$  and independent processes simultaneously and adds them coherently will be developed.

This work was supported by the National Science Foundation, under Grant No. 0969299, by the Emmy-Noether program of the Deutsche Forschungsgemeinschaft (DFG), under Grant No. FI 1593/1-1, by the Alliance Program of the Helmholtz Association, under Grant No. HA216/EMMI, and by the DFG. M. S. acknowledges the DFG for financial support and a scholarship from the Fulbright Foundation. A. B. V. is grateful for support from the Extreme Matter Institute.

---

[1] M. Schulz, R. Moshhammer, D. Fischer, H. Kollmus, D. H. Madison, S. Jones, and J. Ullrich, *Nature (London)* **422**, 48 (2003).  
 [2] T. N. Rescigno, M. Baertschy, W. A. Isaacs, and C. W. McCurdy, *Science* **286**, 2474 (1999).  
 [3] H. Ehrhardt, K. Jung, G. Knoth, and P. Schlemmer, *Z. Phys. D* **1**, 3 (1986).  
 [4] M. Schulz and D. H. Madison, *Int. J. Mod. Phys. A* **21**, 3649 (2006).

[5] L. Ph. H. Schmidt, M. S. Schöffler, K. E. Stiebing, H. Schmidt-Böcking, R. Dörner, F. Afaneh, and Th. Weber, *Phys. Rev. A* **76**, 012703 (2007).  
 [6] J. H. Macek, J. B. Sternberg, S. Y. Ovchinnikov, T.-G. Lee, and D. R. Schultz, *Phys. Rev. Lett.* **102**, 143201 (2009).  
 [7] M. McGovern, C. T. Whelan, and H. R. J. Walters, *Phys. Rev. A* **82**, 032702 (2010).  
 [8] A. Dorn, A. Kheifets, C. D. Schröter, B. Najjari, C. Höhr, R. Moshhammer, and J. Ullrich, *Phys. Rev. Lett.* **86**, 3755 (2001).  
 [9] I. Taouil, A. Lahmam-Bennani, A. Duguet, and L. Avaldi, *Phys. Rev. Lett.* **81**, 4600 (1998).  
 [10] D. Fischer *et al.*, *Phys. Rev. Lett.* **90**, 243201 (2003).  
 [11] M. Schulz, R. Moshhammer, W. Schmitt, H. Kollmus, B. Feuerstein, R. Mann, S. Hagmann, and J. Ullrich, *Phys. Rev. Lett.* **84**, 863 (2000).  
 [12] M. Schulz, M. F. Ciappina, T. Kirchner, D. Fischer, R. Moshhammer, and J. Ullrich, *Phys. Rev. A* **79**, 042708 (2009).  
 [13] W. T. Htwe, T. Vajnai, M. Barnhart, A. D. Gaus, and M. Schulz, *Phys. Rev. Lett.* **73**, 1348 (1994).  
 [14] M. Schulz, T. Vajnai, and J. A. Brand, *Phys. Rev. A* **75**, 022717 (2007).  
 [15] M. S. Schöffler, J. Titze, L. P. H. Schmidt, T. Jahnke, N. Neumann, O. Jagutzki, H. Schmidt-Böcking, R. Dörner, and I. Mančev, *Phys. Rev. A* **79**, 064701 (2009).  
 [16] E. Horsdal, B. Jensen, and K. O. Nielsen, *Phys. Rev. Lett.* **57**, 1414 (1986).  
 [17] J. Pálincás, R. Schuch, H. Cederquist, and O. Gustafsson, *Phys. Rev. Lett.* **63**, 2464 (1989).  
 [18] V. Mergel *et al.*, *Phys. Rev. Lett.* **79**, 387 (1997).  
 [19] V. Mergel, R. Dörner, Kh. Khayyat, M. Achler, T. Weber, O. Jagutzki, H. J. Lüdde, C. L. Cocke, and H. Schmidt-Böcking, *Phys. Rev. Lett.* **86**, 2257 (2001).  
 [20] H. T. Schmidt *et al.*, *Phys. Rev. A* **72**, 012713 (2005).  
 [21] J. H. McGuire, *Electron Correlation Dynamics in Atomic Collisions* (Cambridge University Press, Cambridge, 1997).  
 [22] D. Fischer, M. Schulz, Moshhammer, and J. Ullrich, *J. Phys. B* **37**, 1103 (2004).  
 [23] H. Schmidt-Böcking *et al.*, *Europhys. Lett.* **62**, 477 (2003).  
 [24] A. B. Voitkiv, B. Najjari, and J. Ullrich, *Phys. Rev. Lett.* **101**, 223201 (2008).  
 [25] M. Steck *et al.*, *Nucl. Instrum. Methods Phys. Res., Sect. A* **287**, 324 (1990).  
 [26] R. Dörner, V. Mergel, O. Jagutzki, L. Spielberger, J. Ullrich, R. Moshhammer, and H. Schmidt-Böcking, *Phys. Rep.* **330**, 95 (2000).  
 [27] J. Ullrich, R. Moshhammer, A. Dorn, R. Dörner, L. Schmidt, and H. Schmidt-Böcking, *Rep. Prog. Phys.* **66**, 1463 (2003).  
 [28] D. S. F. Crothers and J. F. McCann, *J. Phys. B* **16**, 3229 (1983).  
 [29] A. B. Voitkiv, *J. Phys. B* **41**, 195201 (2008).  
 [30] A. Salin, *J. Phys. B* **22**, 3901 (1989).  
 [31] M. Schöffler *et al.*, *J. Phys. B* **38**, L123 (2005).  
 [32] L. H. Thomas, *Proc. R. Soc. A* **114**, 561 (1927).  
 [33] J. S. Briggs and K. Taulbjerg, *J. Phys. B* **12**, 2565 (1979).